SLAC-PUB-1745
May 1976

NONRESONANT MULTIBODY PRODUCTION BY e^+e^- ANNIHILATION*

G. J. Feldman
Stanford Linear Accelerator Center
Stanford University, Stanford, California 94305 (USA)

Abstract: We review several aspects of nonresonant multibody production by e^+e^- annihilation. At high energies the ratio of the hadronic cross section to the μ pair production cross section is consistent with being constant; inclusive distributions show approximate Bjorken scaling; and there is strong evidence for jet-like structure. The jets are produced with an angular distribution characteristic of that of pairs of spin 1/2 particles.

Résumé: Différentes propriétés de l'annihilation e^+e^-, en dehors des résonances, sont présentées. A haute énergie le rapport entre la section efficace hadronique et la production de paires de μ est compatible avec une constante; il y a invariance d'échelle à la Bjorken approximative dans les distributions inclusives, et forte évidence de structure en jets. Ces derniers sont produits avec une distribution angulaire caractéristique pour des particules de spin 1/2.

(Invited talk given at the International Meeting on Storage Ring Physics, Flaine, France, February 22 - 28, 1976)

*Work supported by the Energy Research and Development Administration.

INTRODUCTION

We've now heard several talks at this meeting on the various new resonances which have been observed in e^+e^- annihilations. In this talk we will concentrate on some aspects of nonresonant multibody production by e^+e^- annihilations.

The standard model to which we will want to compare our results is the simple quark-parton model.[1] Even though this model is an obvious oversimplification of the underlying physics, we will see that it correctly describes the general features of the data. The model postulates that hadrons are produced as shown in Fig. 1. The virtual photon produces a point-like quark-antiquark pair, each of which miraculously dresses itself to form hadrons. The fragmentation of each quark into hadrons is assumed to be independent of energy and the other quark's fragmentation.

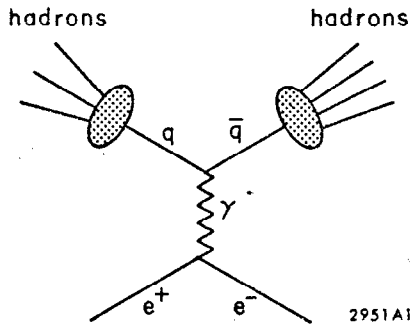

Fig. 1. Hadron production in the simple parton model.

There are four basic predictions of this model which we will examine:

1) The ratio of the hadronic cross section to the μ pair production cross section, R, should be a constant,

$$R = \sum_i q_i^2 \tag{1}$$

where the q's are the quark charges.

2) The inclusive distribution $s\frac{d\sigma}{dx}$ should be independent of s, where $x \equiv 2p/\sqrt{s}$.

3) Hadrons should be produced in a two-jet structure.

4) And, since the quark has spin 1/2, the angular distribution of the jet axis relative to the incident beams should be $1+\cos^2\theta$.

There are some obvious problems with this simple model which should be kept in mind:

1) As the energy increases there will be increased phase space for particles which have comparable momentum and mass. Thus, we would expect Bjorken scaling (prediction 2) to fail for low x particles and for there to be a corresponding logarithmic increase in multiplicity.

2) We know there are thresholds for new channels, or at least new internal degrees of freedom, in the 4 GeV region. There is no reason to expect phenomena above, below, and within this region to be identical. Trivially, if R is not constant, then $s\frac{d\sigma}{dx}$ cannot scale everywhere. Even well above the 4 GeV region there may be problems. Although it may be justifiable to ignore the mass of a 300 MeV quark, it is not at all clear that one can ignore the mass of a 1.5 GeV quark or a 1.8 GeV heavy lepton.

3) Two fractionally charged quarks cannot fragment into integrally charged mesons without some communication between them. Presumably, this

communication occurs through a sea of low momentum parton pairs in such a way as to not greatly affect the high momentum partons.

THE TOTAL CROSS SECTION

All of the data we will discuss today come from the work of the SLAC-LBL magnetic detector collaboration at SPEAR.[2] The detector, shown schematically in Fig. 2, has charge particle detection over about 70% of the solid angle and can

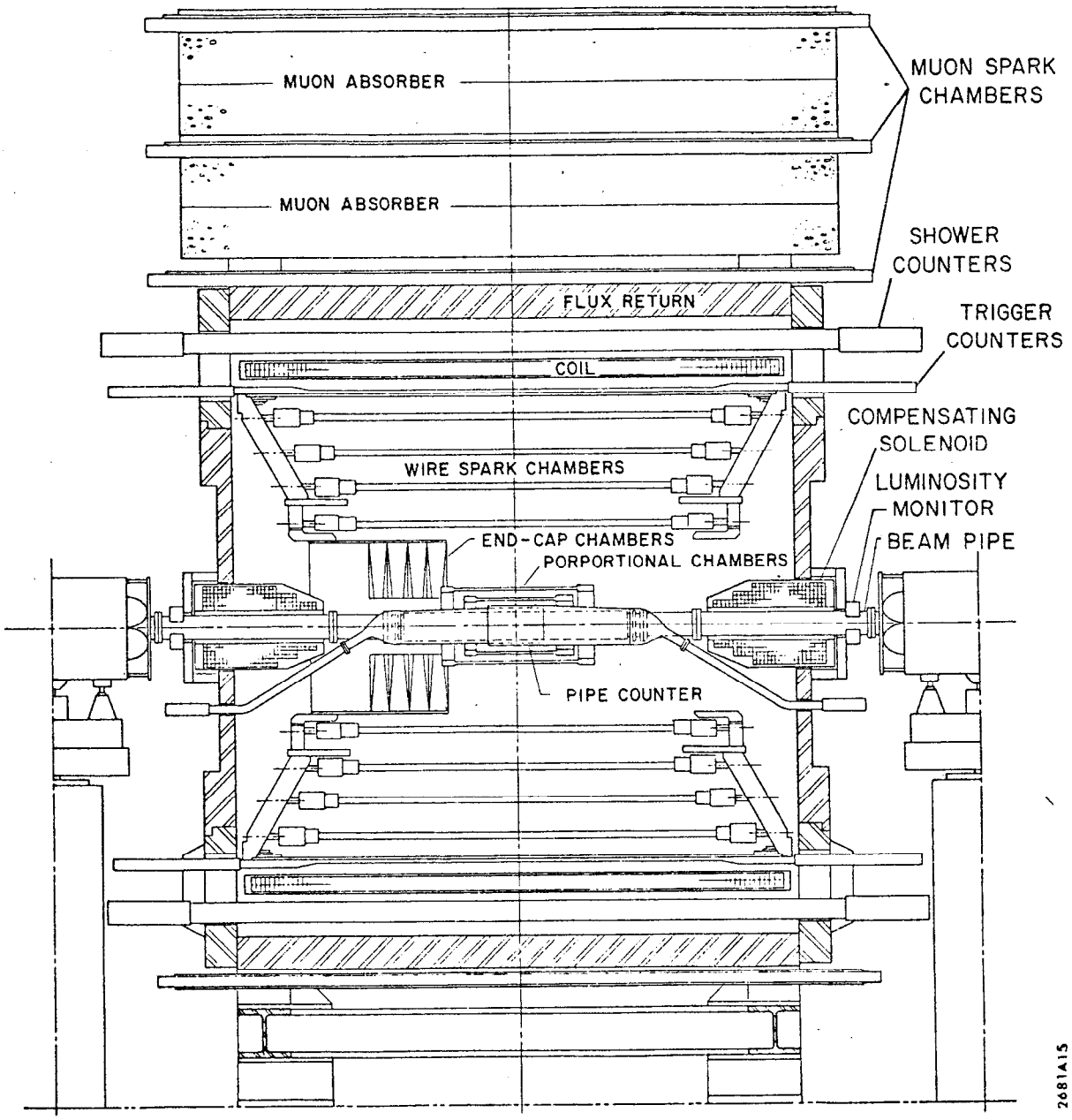

Fig. 2. An elevation view of the SPEAR magnetic detector.

trigger on charged particles in about 65% of the solid angle. The trigger requires at least two charge particles in the sensitive solid angle.[3] Clearly, all of the physical distributions that we present, total cross sections, momentum distributions, angular distributions, etc., must be corrected for the effect of this biased trigger. To do this we perform a Monte Carlo simulation of the final state.

Unfortunately, our knowledge of the final state is imperfect and this leads to an inherent systematic uncertainty, which for the total cross sections is about 15%.[4] The average detection efficiency for hadronic events is shown in Fig. 3.

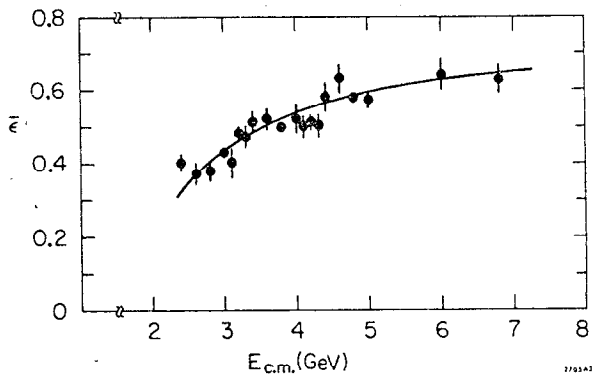

Fig. 3. Average detection efficiency versus energy for hadronic events. The points are fits of the Monte Carlo calculations to the observed multiplicities. The curve is a smooth fit to the points.

Figure 4 gives the ratio, R, of the hadronic to μ pair production cross sections as a function of center of mass energy. The error bars allow for an 8 to 10% point to point systematic error, but do not include the overall 15% systematic uncertainty. Most of the points have been corrected for detection efficiency by the use of the smooth curve shown in Fig. 3. The data have also been corrected for backgrounds due to beam-gas interactions, leptonic two-photon processes, and radiative effects.

Three separate regions are clearly visible in Fig. 4. There are two plateau regions where R is consistent with being a constant and a transition region between them which contains a great deal of structure.[5] R is consistent with being about two and a half from 2.4 to 3.4 GeV and is consistent with being about twice as large above 4.8 GeV.

This behavior is consistent with the parton model if new degrees of freedom are being excited in the 4 GeV region, such as new quarks. New leptons produced

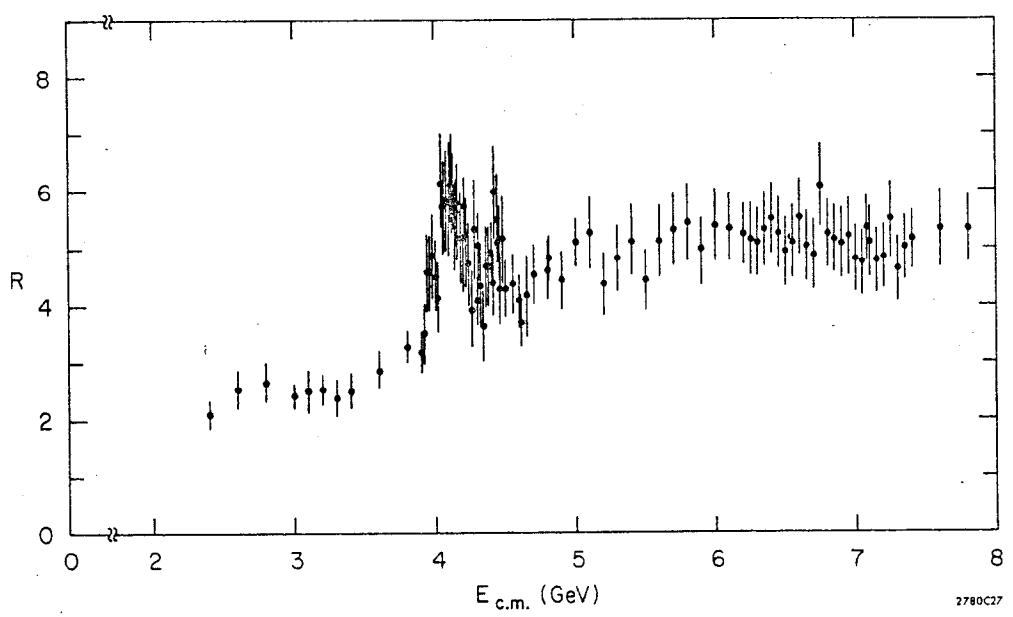

Fig. 4. The ratio of the hadronic to μ pair production cross sections versus energy.

in the 4 GeV region would also add one unit each to R since their decays would look like hadronic events. There is now a great deal of evidence that at least one new lepton is being produced in this region.[6] If we assume that R as determined by Eq. (1) is uniformly too low by a factor of 1.25 (for quarks, but not leptons) then Fig. 4 is in perfect agreement with three quarks in the lower plateau and four quarks plus one new lepton in the higher plateau.

INCLUSIVE DISTRIBUTIONS

The inclusive distribution $s\frac{d\sigma}{dx}$ for three energies is shown in Fig. 5.[7] Since the integral of this distribution is proportional to R times the average charged multiplicity, the 3 GeV data cannot agree with the higher energy data everywhere. The rather surprising thing is that all the data approximately scale for $x > 0.5$. This means that if the distributions corresponding to the lower plateau, the "old physics", scale, then all of the contribution of the "new physics" is at $x < 0.5$.

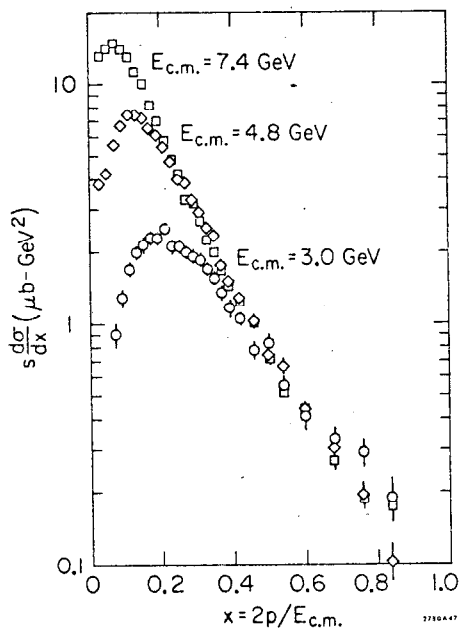

Fig. 5. s dσ/dx versus x for three energies.

Once we are in the upper plateau, there is approximate scaling for $x > .2$. The lack of scaling at low x is at least partially due to the finite particle masses.

A more sensitive way to investigate scaling is to plot $s\frac{d\sigma}{dx}$ versus energy for different x regions, as shown in Fig. 6. At $x = 0.1$ there is no scaling at any energy, while at $x \geq 0.5$ there is approximate scaling at all energies. In the intermediate x values, one can see the approach to scaling as a function of energy. The data around 4 GeV are high for $x \leq 0.4$. This can also be seen in Fig. 7, where the shape of the $4.0 < E_{c.m.} < 4.4$ GeV spectrum is clearly anomalous. This distribution is consistent with there being a healthy dose of new physics in this region.

MEAN MULTIPLICITIES AND ENERGIES

There are several quantities which can be derived from the inclusive distributions and which help to give a global picture of the events. Figure 8 shows the mean charged multiplicity versus energy, with the latter plotted on a logarithmic scale. The data are consistent with a logarithmic increase with energy, as is seen in other reactions. As we mentioned earlier, this is consistent with the parton model if the increased multiplicity comes from the low x region where masses are important.

Figure 9 shows the average energy per charged track assuming pion masses. The data are roughly consistent with a linear rise with a possible leveling off and change of slope in the 4 GeV region.

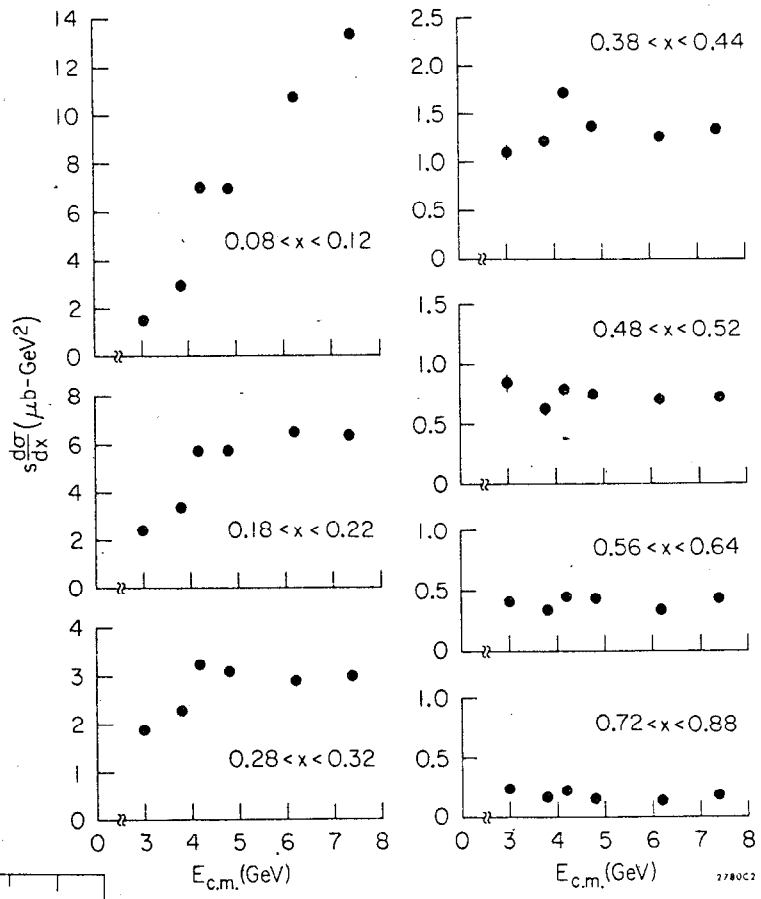

Fig. 6. s $d\sigma/dx$ versus energy for several x intervals.

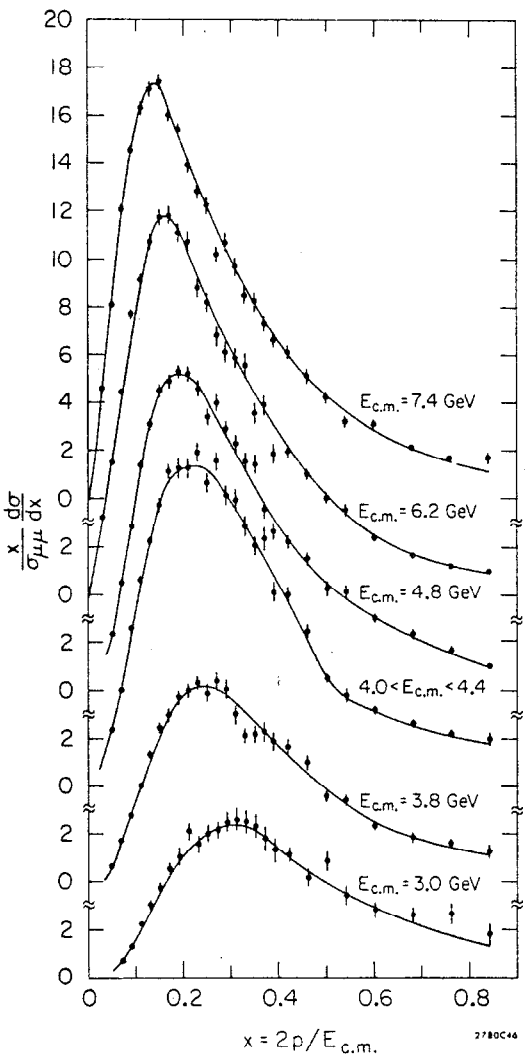

Fig. 7. $(x/\sigma_{\mu\mu})$ $(d\sigma/dx)$ versus x for various energies.

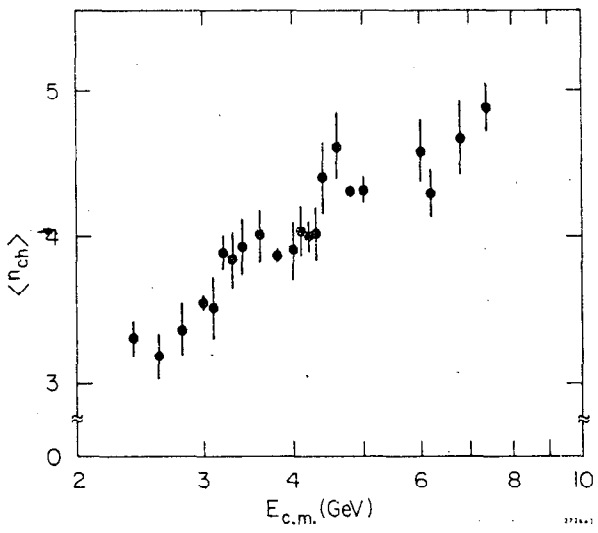

Fig. 8. Mean charged multiplicity versus energy.

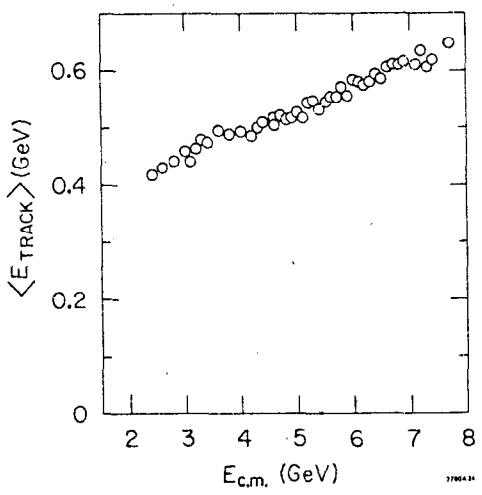

Fig. 9. Mean energy per charged particle (assuming a pion mass) versus energy.

Combining Figs. 8 and 9 we can obtain the average fraction of energy which goes into charged particles. This is shown in Fig. 10. Again we have assumed that all detected charged particles are pions. The fraction decreases from about 0.60 to 0.50. If only neutral and charged pions were produced, then we would expect this fraction to be 0.67 in a statistical model. The difference between 0.67 and 0.60 can probably be accounted for by a reasonable amount of η, kaon, and nucleon production, but the fall to 0.50 is harder to understand unless energy is being taken away by neutrinos.[8] We do not yet have sufficient knowledge of the details of the final state to understand this fraction. However, regardless of its origin, scaling implies that it should be a constant, and the data suggest that it may level off above 5 GeV.

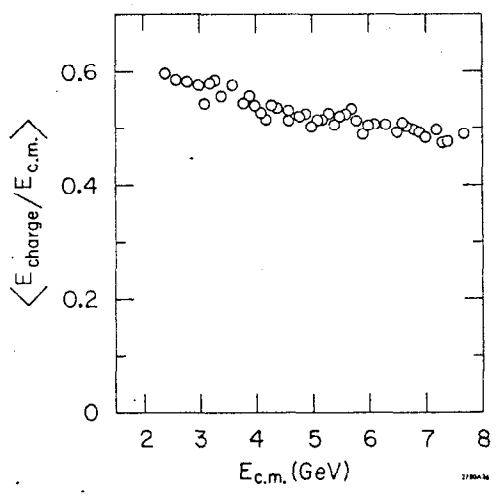

Fig. 10. Ratio of energy carried by charged particles to the total energy. All charged particles are assumed to be pions.

JET STRUCTURE[9]

The key to searching for jets lies in the definition of jet structure. One can characterize jet structure as the tendency for the transverse momentum to be limited with respect to some axis. This definition allows us to quantify the amount of jet-like behavior by a single parameter: the average transverse momentum to the jet axis. (A second parameter will be needed to specify the angular distribution of the jet axis.)

The procedure for finding jets was developed by Gail Hanson starting from a suggestion by Bjorken and Brodsky.[10] In words, the procedure is

a) Find for each event the axis which minimizes the sum of the squares of transverse momenta to it. This axis will be defined as the reconstructed jet axis.

b) Construct a quantitative measure of the amount of jet-like structure by comparing the relative amount of transverse momenta to the jet axis to the amount of transverse momenta to orthogonal axes.

c) Perform Monte Carlo simulations to evaluate the significance of the results.

The jet axis is found mathematically for each event by constructing the tensor

$$T_{\alpha\beta} = \sum_i \left(\delta_{\alpha\beta} p_i^2 - p_\alpha^i p_\beta^i\right) \tag{2}$$

where the summation is over all detected charged particles and α and β are Cartesian coordinates. This tensor is analogous to a moment of inertia tensor. Only events with three or more detected particles are used to avoid some background problems.

The tensor is diagonalized to yield three eigenvectors and three eigenvalues, λ_1, λ_2, and λ_3. The eigenvalues are the sum of the squares of the transverse momenta to the eigenvector directions. The smallest eigenvalue, λ_3, is the minimum sum of transverse momenta to any axis, and thus its associated eigenvector is the reconstructed jet axis.

To measure how jet-like an event is, we define the sphericity, S,

$$S \equiv \frac{3\lambda_3}{\lambda_1+\lambda_2+\lambda_3} = \frac{3\left(\sum p_{\perp i}^2\right)_{min}}{2\sum p_i^2} \quad . \tag{3}$$

For each event the sphericity is between 0 and 1.

Finally, to interpret the results, two types of Monte Carlo simulations were performed. In the first, the phase space model, events were simulated with the particles' momentum distributions given by invariant phase space. The mean multiplicity of produced particles and the ratio of charged to neutral particles were set in the Monte Carlo to match the observed mean charged multiplicity and average momentum. The second model, the jet model, differed only in that a matrix element squared,

$$|M|^2 = e^{-\left(\sum p_{\perp i}^2\right)/2r^2} \tag{4}$$

was inserted. The summation is taken over all of the produced particles, $p_\perp$ is the momentum transverse to the produced jet axis, and r is a free parameter which can be adjusted to give a desired mean transverse momentum.

In both models all particles were assumed to be pions. Calculations done with the addition of kaons, η's, and nucleons give substantially the same results.

SPHERICITY

The mean observed sphericity as a function of energy is shown in Fig. 11. It is fairly constant between 3.0 and 4.8 GeV, but is significantly lower at 6.2 and 7.4 GeV. The expected mean observed sphericity based on the phase space model is given by the dashed line. It rises as a function of energy in sharp contrast to the data. The rise predicted by this model is due to the increase in multiplicity with energy and will occur in any uncorrelated model. The solid curve shows the results of the jet model. At 7.4 GeV the model is fit to agree with the mean observed sphericity. At the other energies the model is adjusted to give the same mean transverse momentum to the jet axis (3.15 MeV/c) as is deduced from the model at 7.4 GeV. This procedure gives a reasonable description of the data everywhere.

Figure 12 shows observed sphericity distributions at three energies. At 3.0 GeV, the phase space and jet models are essentially identical and both describe the distribution well. However, at 6.2 and 6.4 GeV, only the jet model provides a reasonable description of the data.

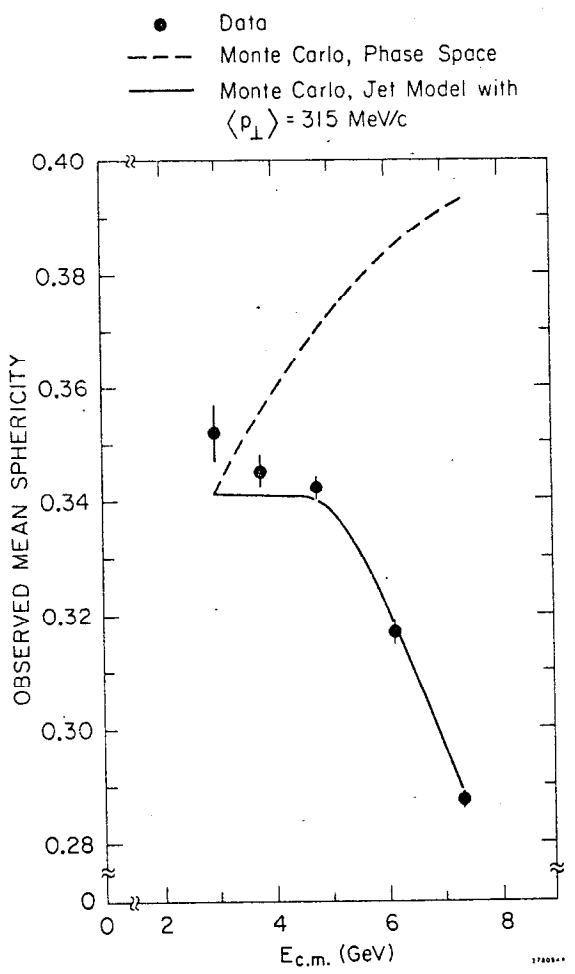

Fig. 11. Observed mean sphericity versus energy. The dashed curve represents the phase space model Monte Carlo calculation and the solid curve represents the jet model calculation with $\langle p_\perp \rangle$ = 315 MeV/c.

ALTERNATE EXPLANATIONS

These distributions provide the basic evidence for jet-like structure in e^+e^- annihilations. They show that at high energy the data are not described well by invariant phase space but can be described by a model in which the transverse momentum is limited. We will now consider some alternative explanations for this behavior.

The inclusive x distribution at 7.4 GeV does not agree with the predictions of the phase space model. This can be seen in Fig. 13 where the 7.4 GeV data from Fig. 5 are replotted along with the Monte Carlo distributions. This disagreement is to be expected given the existence of jets, but a legitimate

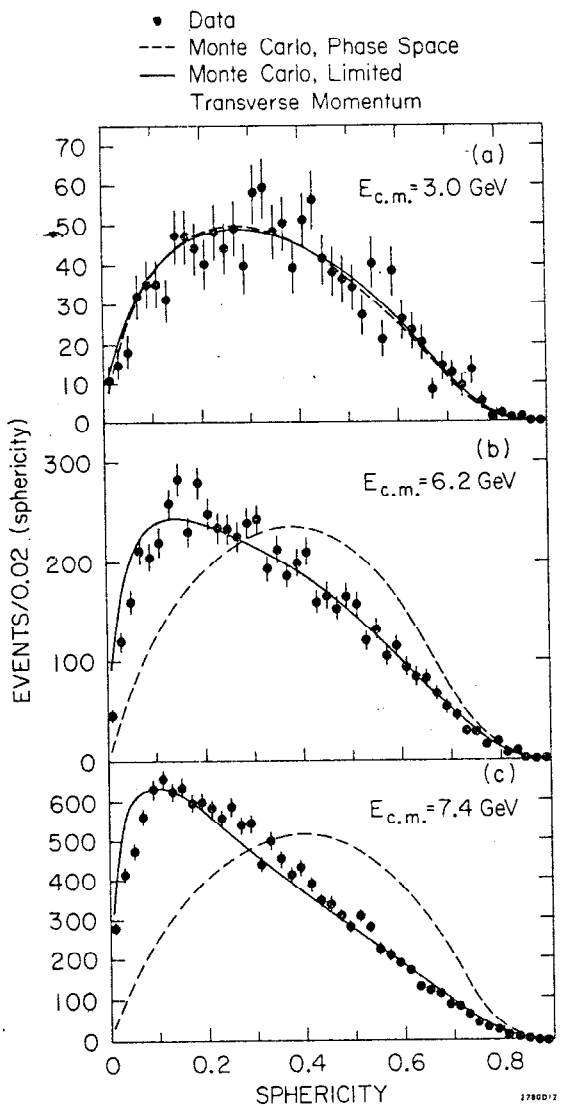

Fig. 12. Observed sphericity distributions at three energies. The dashed curve represents the phase space model Monte Carlo calculation and the solid curve represents the jet model calculation with $\langle p_\perp \rangle$ = 315 MeV/c.

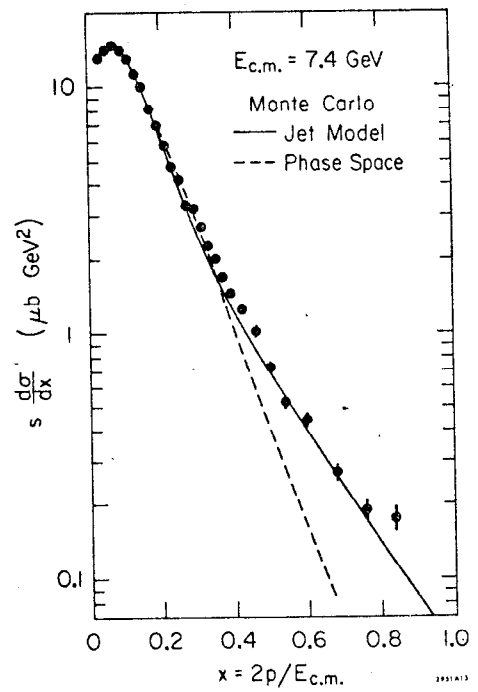

Fig. 13. s $d\sigma/dx$ versus x for 7.4 GeV. The dashed and solid curves represent the phase space model and jet model calculations, respectively.

question can be asked: Is the existence of extra high momentum tracks sufficient to give jet-like sphericity distributions? The answer is no, as illustrated by Fig. 14. Here the data at 7.4 GeV have been divided into two sets, one in which there is an observed particle with x > 0.4, and one in which there is not. The latter set is in good agreement with the phase space momentum distribution, while the former set has an enriched sample of high momentum tracks and is thus closer to the (renormalized) phase space momentum distribution. In both cases the phase space sphericity distributions fail to describe the data, while the jet model distributions are reasonably close.

Another alternative explanation is that the jet structure is caused by the production of two heavy mesons which decay. This process might dominate at present energies, but slowly die out at higher energies. We have not found any data to support this explanation. Figure 15 shows the distribution of observed jet masses, where the jet mass is defined by constructing a plane perpendicular to the reconstructed jet axis and calculating the invariant mass of the observed particles on either side of the plane. There are two discrete bins in Fig. 15(a) which

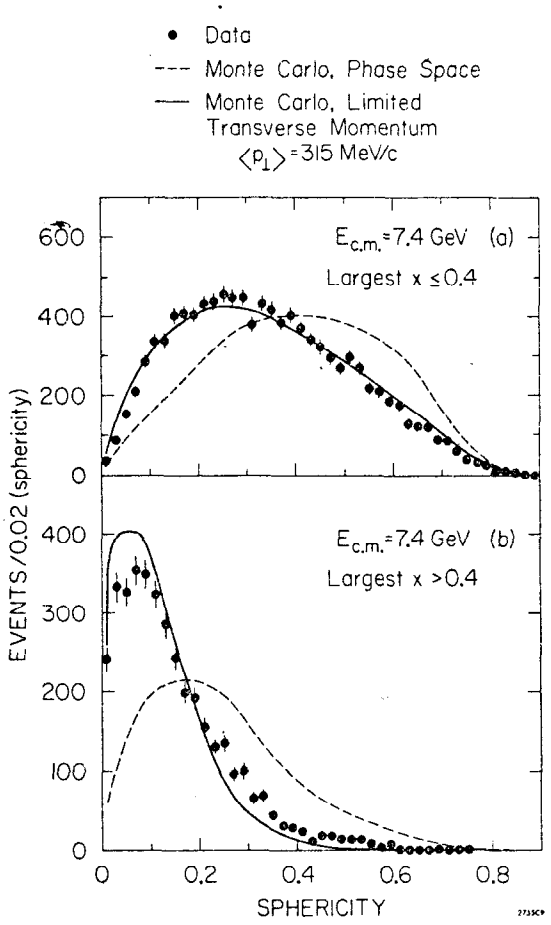

Fig. 14. Observed sphericity distributions at 7.4 GeV for (a) events in which all detected particles have $x < 0.4$ and (b) events in which at least one particle is detected with $x > 0.4$. The dashed and solid curves represent the phase space model and jet model calculations, respectively.

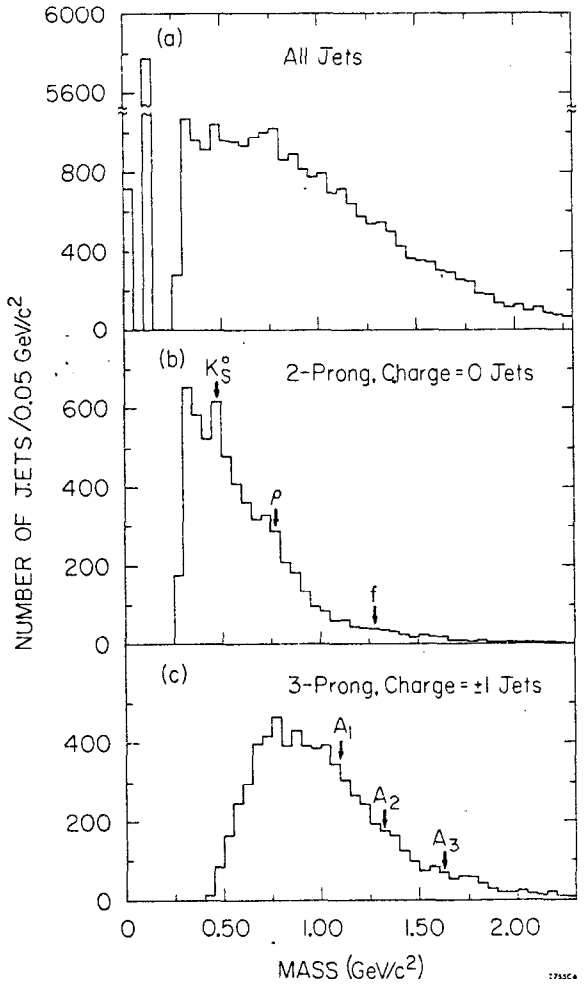

Fig. 15. Observed distribution of jet masses at 7.4 GeV for (a) all jets, (b) 2-prong charge 0 jets, and (c) 3-prong charge 1 jets. Pion masses have been assumed for all particles. The arrows indicate the positions of known resonances.

correspond to the detection of zero and one charged particles. When two or more charged particles are detected in the jet there is a smooth continuum of masses which is flat from threshold to about 750 MeV and then decreases. In Figs. 15(b) and 15(c) where two and three prong jets have been isolated, there is evidence for K_S^0's and ρ's but f and A mesons are not evident. In all there does not seem to be any evidence for copious resonance production.

JET ANGULAR DISTRIBUTIONS

Under the assumption of one photon exchange all angular distributions, whether they be of inclusive hadrons or of the jet axis, must be of the form

$$\frac{d\sigma}{d\theta} \propto 1 + \alpha \cos^2\theta + P^2 \alpha \sin^2\theta \cos^2\phi \qquad (5)$$

where

$$\alpha = \frac{\sigma_T - \sigma_L}{\sigma_T + \sigma_L} \quad , \tag{6}$$

σ_T and σ_L are transverse and longitudinal cross sections, θ is the polar angle to the beam, P is the transverse beam polarization, and ϕ is the azimuthal angle measured from the plane of the ring.[11] The only parameter in Eq. (5), α, can be measured even if P is zero, so the transverse polarization gives no new theoretical information. However, since the SPEAR magnetic detector measures a portion of the θ region, but is almost unbiased in ϕ, the polarization is extremely important experimentally.

Figure 16 shows the observed azimuthal angle of the jet axis at 7.4 GeV, where polarization has been observed, and at 6.2 GeV, where polarization is absent due to a depolarizing resonance at that energy.[12] The data at 7.4 GeV show a clear azimuthal dependence from which an α for the jet axis can be deduced with the aid of the jet model simulation,

$$\alpha_{jet} = 0.78 \pm 0.12 \ , \tag{7}$$

where the error reflects only the statistical uncertainty. This value is close to what one expects for jets originating from spin 1/2 partons, α=1, and is completely incompatible with the prediction of spin 0 partons, α=-1.

The jet model also produces a good description of the inclusive hadron angular distribution. Figure 17 shows α versus x for inclusive hadrons and the prediction of the jet model with $\alpha_{jet} = 0.78 \pm 0.12$. The change from isotropic particle production at low x to muon-like distributions at high x is reproduced.

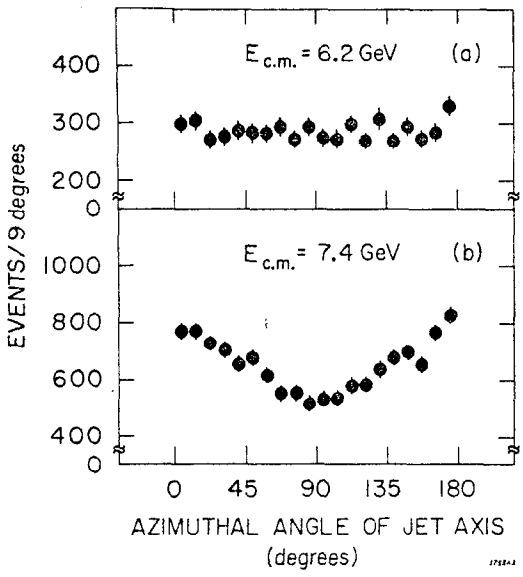

Fig. 16. Observed distribution of the jet axis azimuthal angle for $|\cos\theta| < 0.6$ at 6.2 and 7.4 GeV.

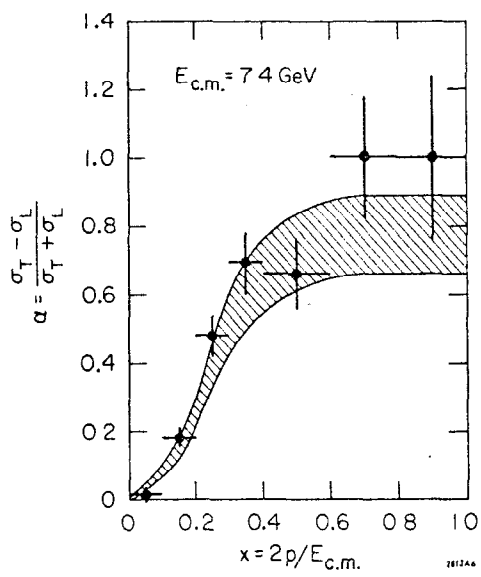

Fig. 17. Observed inclusive α versus x at 7.4 GeV. The shaded band represents the prediction of the jet model Monte Carlo calculation.

A LOOK FORWARD

Since part of this meeting will be devoted to discussing plans for higher energy storage rings, it is appropriate to try to extrapolate our findings at present energies to the next generation of machines. Figure 18 shows the mean sphericity at 30 GeV as predicted by the phase space and jet models.[14] The distributions are almost completely disjoint. Jet structure will be completely obvious and no fancy sphericity analysis will be necessary to establish it.

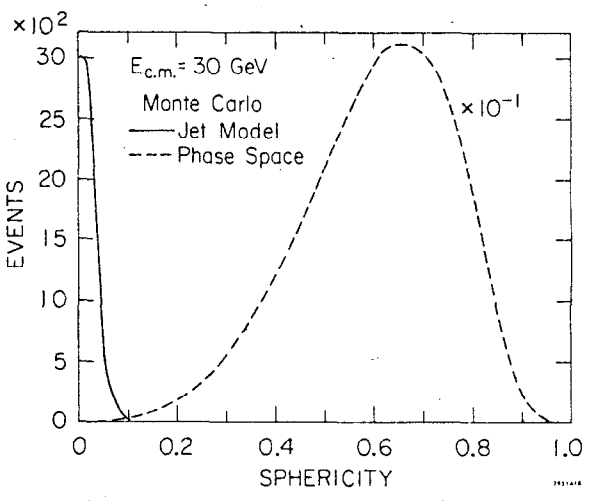

Fig. 18. Predicted sphericity distributions at 30 GeV by the phase space and jet model Monte Carlo calculations.

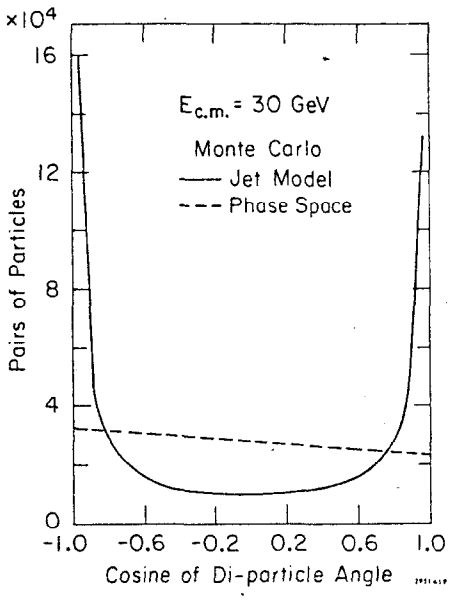

Fig. 19. Predicted distribution of the cosine of the angle between any two particles at 30 GeV by the phase space and jet model Monte Carlo calculations.

This is further illustrated by Fig. 19, where the cosine of the angle between any pair of particles is plotted. The practical problem illustrated by this figure is that one must exercise some care in designing experimental apparatus for PEP or PETRA. For example, a large Cerenkov cell will be useless if there is almost always more than one particle in it.

Practical problems aside, it is clear that 30 GeV will be a fruitful energy at which to study the dynamics of e^+e^- annihilation.

REFERENCES

1. No attempt will be made here to review the theoretical literature. For a discussion of the basic model see J. D. Bjorken, Phys. Rev. 179, 1547 (1969); S. D. Drell, D. J. Levy, and T.-M. Yan, Phys. Rev. D 1, 1617 (1970); and R. P. Feynman, Photon-Hadron Interactions (W. A. Benjamin, Reading, Mass., 1972).
2. The members of the SLAC-LBL collaboration are G. S. Abrams, A. M. Boyarski, M. Breidenbach, F. Bulos, W. Chinowsky, G. J. Feldman, C. E. Friedberg, D. Fryberger, G. Goldhaber, G. Hanson, D. L. Hartill, B. Jean-Marie, J. A. Kadyk, R. R. Larsen, A. M. Litke, D. Lüke,

B. A. Lulu, V. Lüth, H. L. Lynch, C. C. Morehouse, J. M. Paterson, M. L. Perl, F. M. Pierre, T. P. Pun, P. A. Rapidis, B. Richter, B. Sadoulet, R. F. Schwitters, W. Tanenbaum, G. H. Trilling, F. Vannucci, J. S. Whitaker, F. C. Winkelmann, and J. E. Wiss.

3. For a description of the detector and the trigger see J.-E. Augustin et al., Phys. Rev. Lett. 34, 233 (1975) and G. J. Feldman and M. L. Perl, Phys. Rep. C 19, 233 (1975), Appendix A.

4. For a discussion of the event selection and Monte Carlo efficiency corrections see J.-E. Augustin et al., Phys. Rev. Lett. 34, 764 (1975) and G. J. Feldman and M. L. Perl, Phys. Rep. C 19, 233 (1975), Appendix B.

5. R. F. Schwitters, these proceedings and J. Siegrist et al., Phys. Rev. Lett. 36, 700 (1976).

6. M. L. Perl, these proceedings and M. L. Perl et al., Phys. Rev. Lett. 35, 1489 (1975).

7. For experimental details see R. F. Schwitters, Proceedings of the 1975 International Symposium on Lepton and Photon Interactions at High Energies (Stanford Linear Accelerator Center, Stanford, California, 1975; W. T. Kirk, editor).

8. See Feldman and Perl, Ref. 4.

9. G. Hanson et al., Phys. Rev. Lett. 35, 1609 (1975).

10. J. D. Bjorken and S. J. Brodsky, Phys. Rev. D 1, 1416 (1970).

11. V. N. Baier, in Physics with Intersecting Storage Rings, Proceedings of the International School of Physics "Enrico Fermi," Course XLVI, edited by B. Touschek (Academic, New York, 1971), pp. 1-49; and F. J. Gilman, private communication.

12. J. G. Learned, L. K. Resvanis, and C. M. Spencer, Phys. Rev. Lett. 35, 1688 (1975).

13. R. F. Schwitters, Phys. Rev. Lett. 35, 1320 (1975).

14. G. Hanson and P. Oddone, Proceedings of the 1975 PEP Summer Study, Stanford Linear Accelerator Center report number SLAC-190, p. 8.